

Jarid1b targets genes regulating development and is involved in neural differentiation

Sandra U. Schmitz^{1,2*}, Mareike Albert^{1,2*}, Martina Malatesta^{1,2}, Lluís Morey^{1,2,5}, Jens V. Johansen^{1,3}, Mads Bak⁴, Niels Tommerup⁴, Iratxe Abarategui^{1,2}, and Kristian Helin^{1,2}

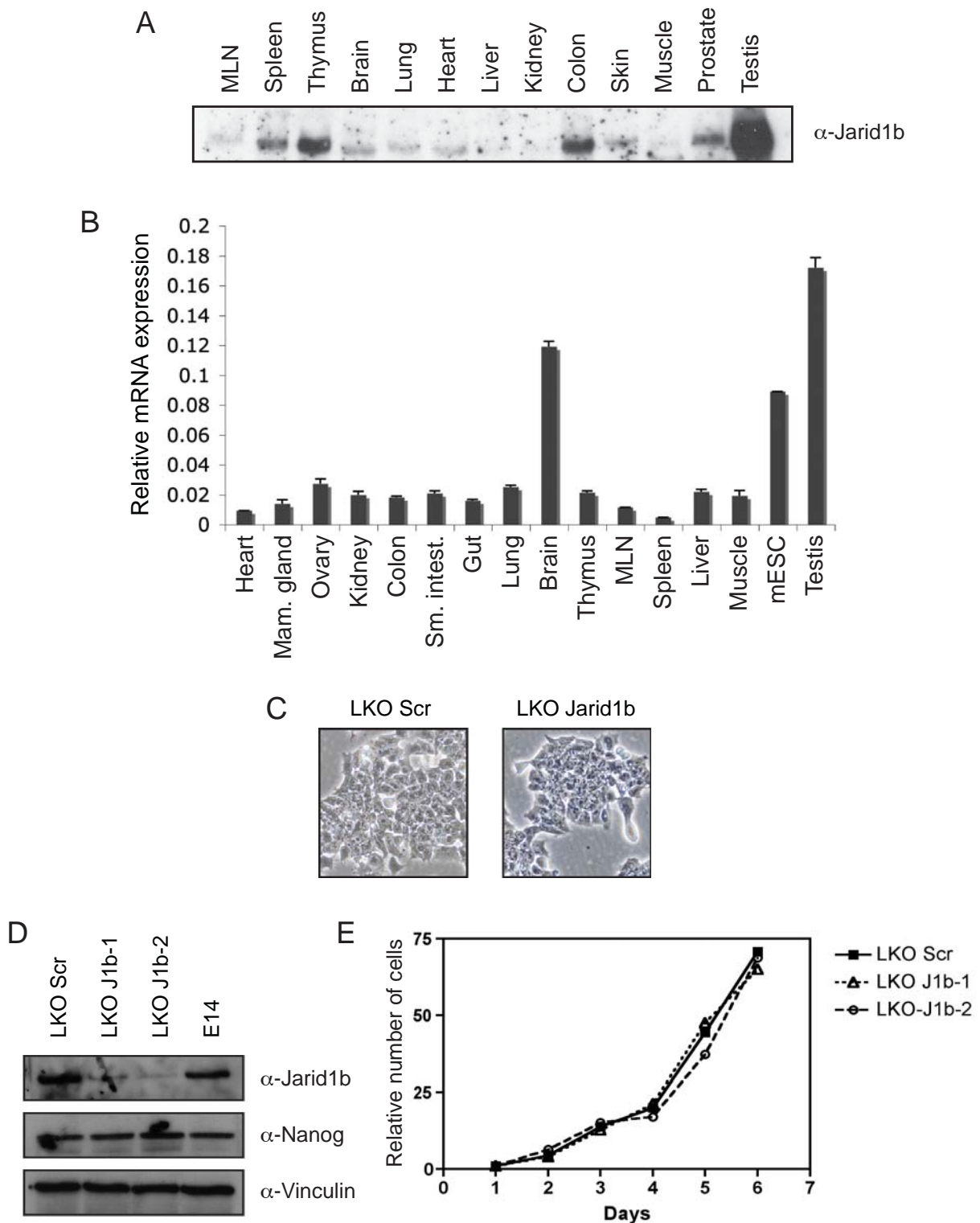
¹Biotech Research and Innovation Centre (BRIC) and ²Centre for Epigenetics, University of Copenhagen, Ole Maaløes Vej 5, 2200 Copenhagen, Denmark.

³The Bioinformatics Centre, Department of Biology, University of Copenhagen, Ole Maaløes Vej 5, 2200 Copenhagen, Denmark.

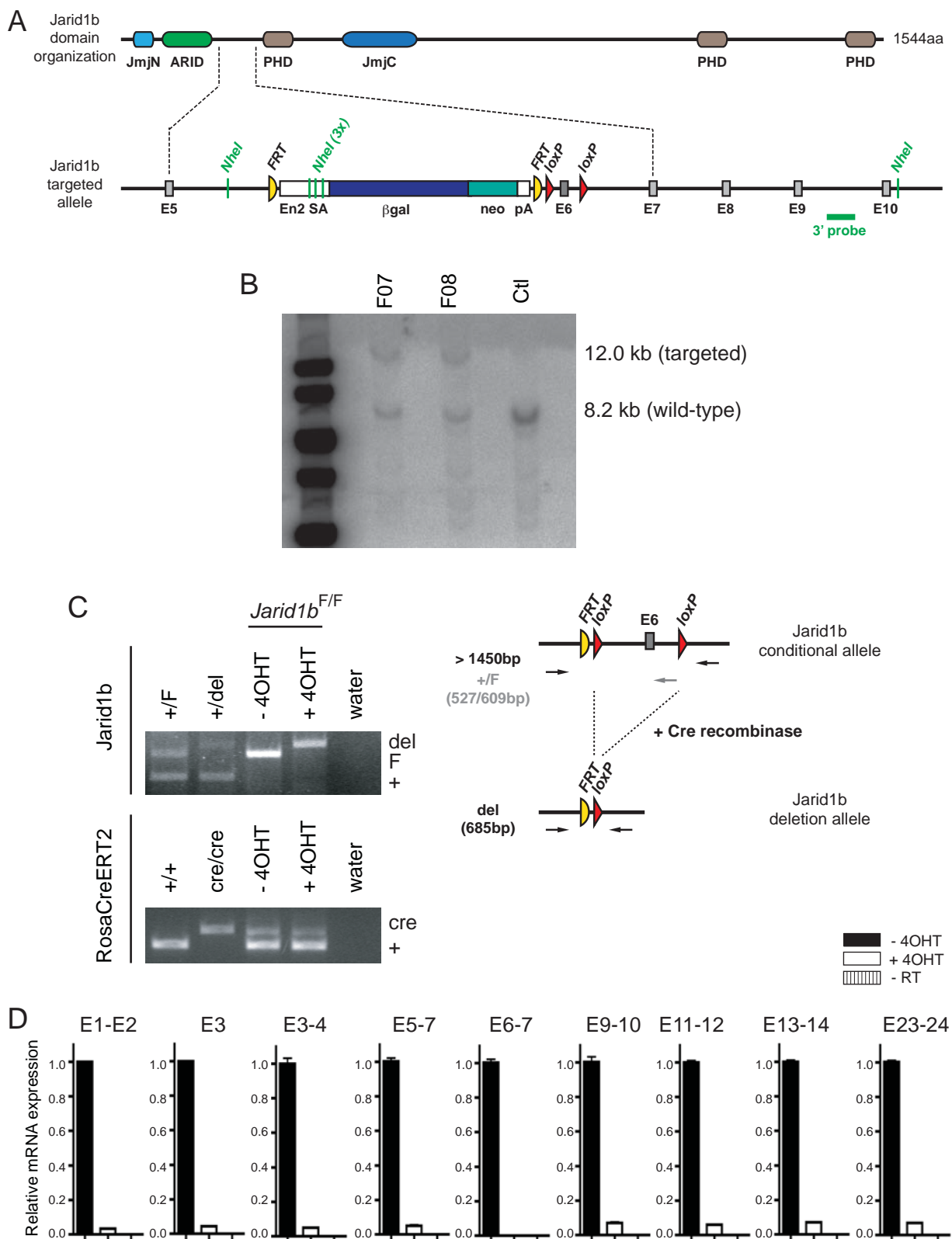
⁴Wilhelm Johannsen Centre for Functional Genome Research, Department of Cellular and Molecular Medicine, University of Copenhagen, Blegdamsvej 3, 2200 Copenhagen N, Denmark.

⁵Present address: Center for Genomic Regulation, c/ Dr. Aiguader 88, 08003 Barcelona, Spain

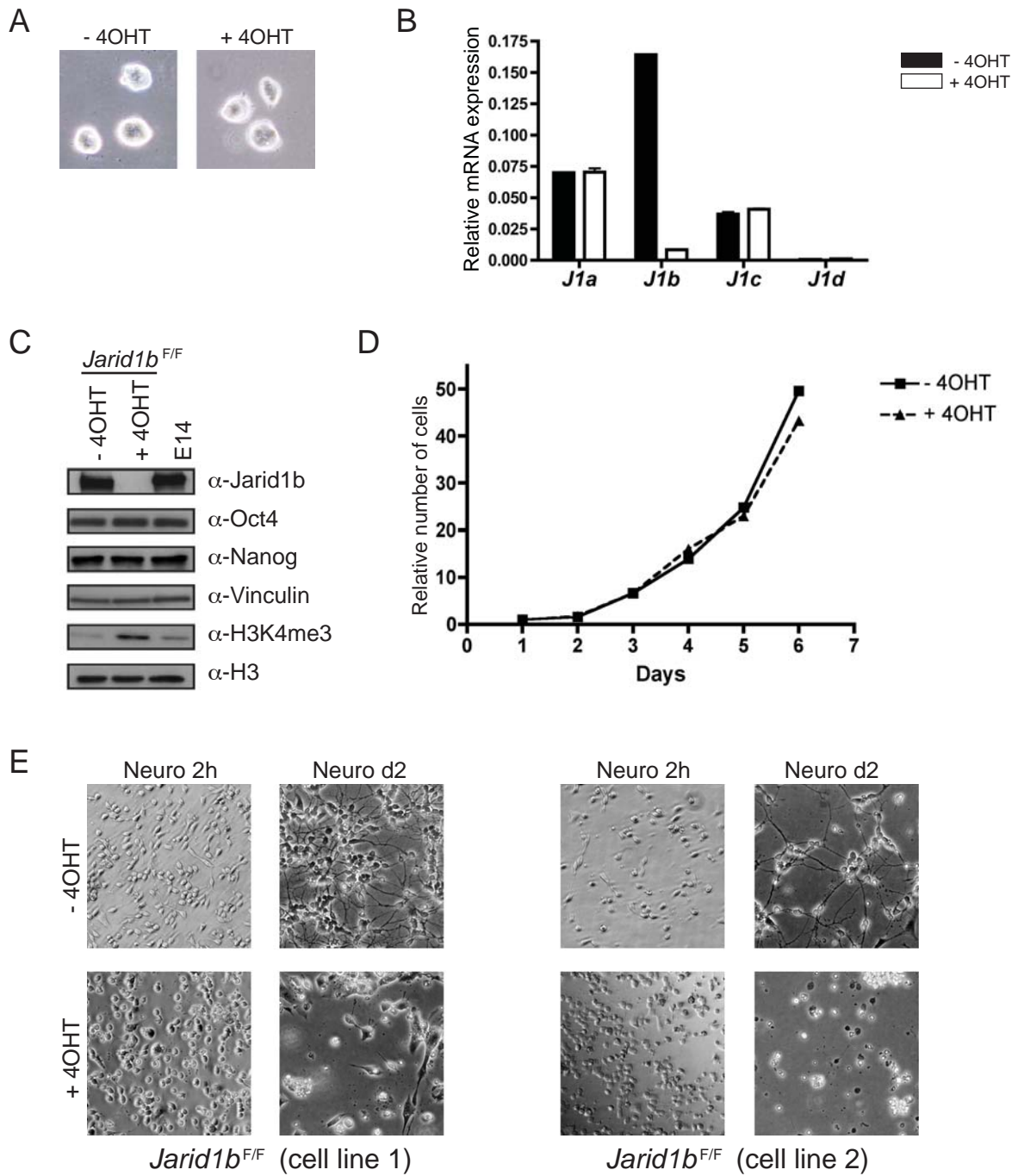
* These authors contributed equally to this work.



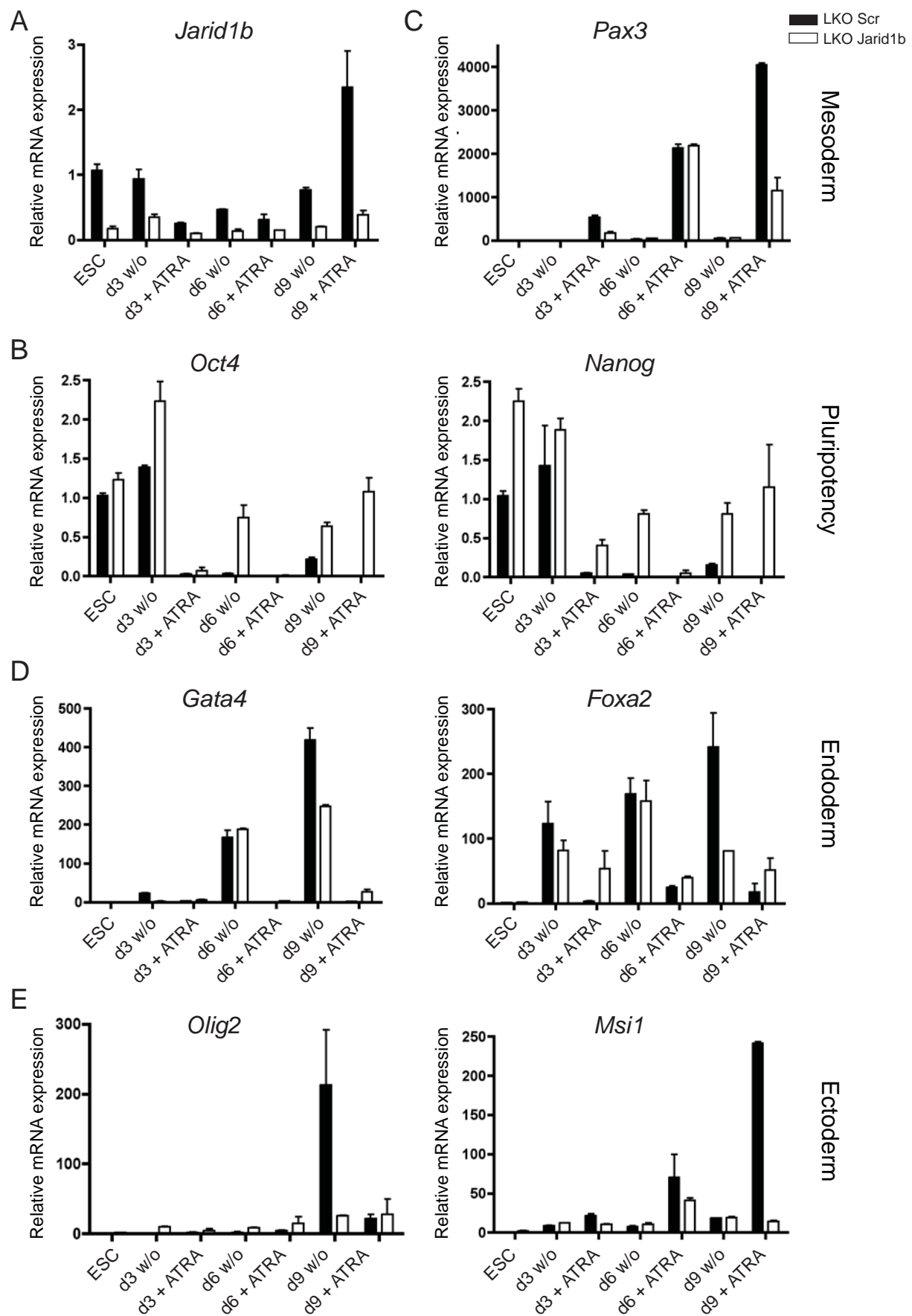
Supplementary Figure 1. Jarid1b expression and characterization of Jarid1b knockdown ESCs. **(A)** Immunoblot showing Jarid1b levels in mouse organs. MLN: mesenteric lymph nodes. **(B)** Expression of *Jarid1b* in different mouse organs determined by quantitative RT-PCR analysis (normalized to *Rplp0* levels). **(C)** Light microscope images of control (Scr) and Jarid1b knockdown ESCs. **(D)** Immunoblots of LKO Scr, LKO Jarid1b (J1b-1 and J1b-2) and E14 ESC lines showing Jarid1b knockdown efficiency and Nanog levels. Vinculin was used as loading control. **(E)** Growth curve of LKO Scr and LKO Jarid1b (J1b-1 and J1b-2) ESC lines.



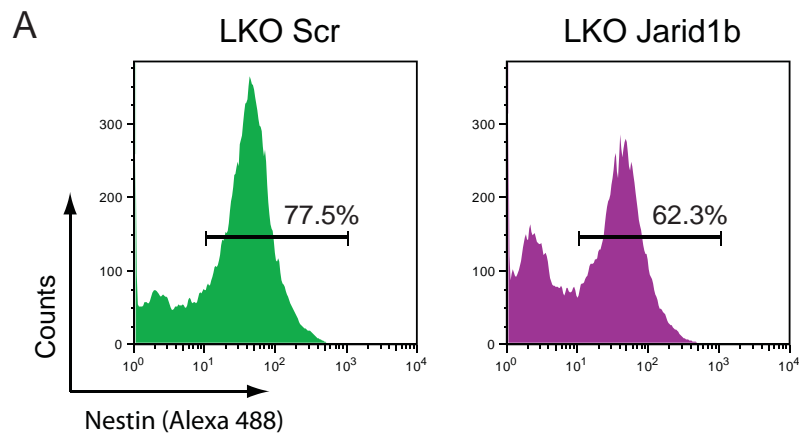
Supplementary Figure 2. Knockout strategy for conditional *Jarid1b* deletion. **(A)** Overview of the *Jarid1b* locus and the targeting cassette. **(B)** Southern blot of two targeted ESC lines (F07 and F08) confirming integration of the *Jarid1b* targeted allele into the correct locus. Genomic DNA was digested with *NheI*. **(C)** Agarose gels showing PCR amplification of *Jarid1b* wild-type, floxed and deletion alleles (top panel) and expression of Cre (bottom panel). -/+ 4OHT samples represent *Jarid1b*^{F/F}; *Rosa26*::*CreERT2* ESCs. A schematic overview of the genotyping strategy is presented on the right. **(D)** Expression of *Jarid1b* in control (-4OHT) and *Jarid1b* knockout ESCs (+4OHT) determined by quantitative RT-PCR analysis (normalized to β -actin levels). Primers were designed to cover exons encoding the following functional domains: JmjN (E1-2), ARID (E3 and E3-4), JmjC (E11-12 and E13-14) and PHD2 (E23-24).



Supplementary Figure 3. *Jarid1b* knockout ESCs can be maintained but not differentiated into neurons. **(A)** Light microscope images of control (- 4OHT) and *Jarid1b* knockout ESCs (+ 4OHT). **(B)** Expression of *Jarid1* family members in control (- 4OHT) and *Jarid1b* knockout ESCs (+ 4OHT) determined by quantitative RT-PCR analysis (relative to β -actin levels). **(C)** Immunoblots of control and *Jarid1b* knockout ESC lines probed for Jarid1b, the stem cell markers Oct4 and Nanog, Vinculin (loading control), H3K4me3 and H3 (loading control). **(D)** Growth curve of control (- 4OHT) and *Jarid1b* knockout ESCs (+ 4OHT). **(E)** Light microscope images of control (- 4OHT) and *Jarid1b* knockout (+ 4OHT) ESCs differentiated to neural progenitor cells (Neuro 2h) and early neurons (Neuro d2). Two independent *Jarid1b* conditional ESC lines are shown (left and right panel).



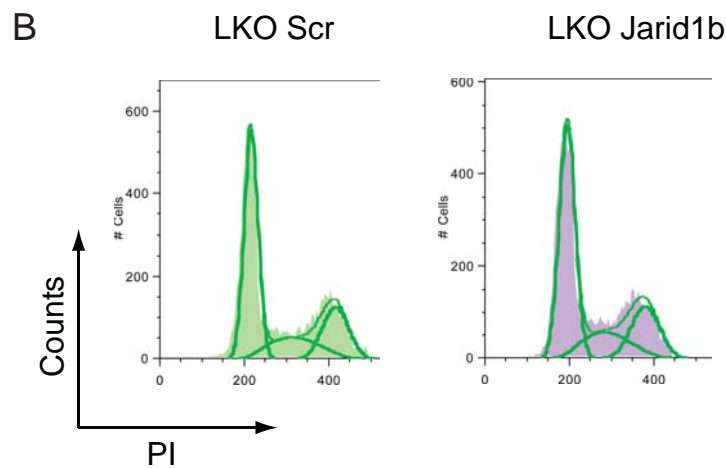
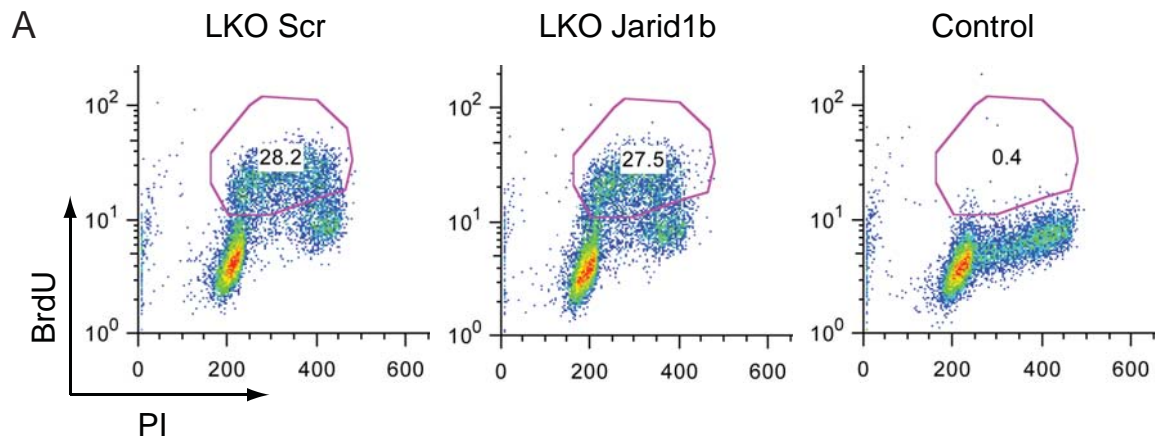
Supplementary Figure 4. Impaired induction of differentiation markers during EB formation of *Jarid1b* knockdown ESCs. Expression of (A) *Jarid1b*, (B) stem cell, (C) mesoderm, (D) endoderm and (E) ectoderm marker genes during embryoid body formation with or without ATRA pulsing analyzed at day 0, 3, 6 and 9, determined by quantitative RT-PCR analysis (normalized to *Rplp0* levels) in control (Scr) and *Jarid1b* knockdown ESCs.



B

Nestin pos	Exp. 1	77.5	62.3	
	Exp. 2	63.3	44.7	
	Exp. 3	68.5	50.1	
Average		69.77	52.37	p=0.004

Supplementary Figure 5. Depletion of Jarid1b leads to a reduced number of Nestin-expressing cells during EB differentiation. **(A)** Histogram plots of flow cytometry analysis of cells from day 8 dissociated embryoid bodies (Bibel et al, 2007), stained with an anti-Nestin antibody. **(B)** Quantification of results obtained in three independent experiments.

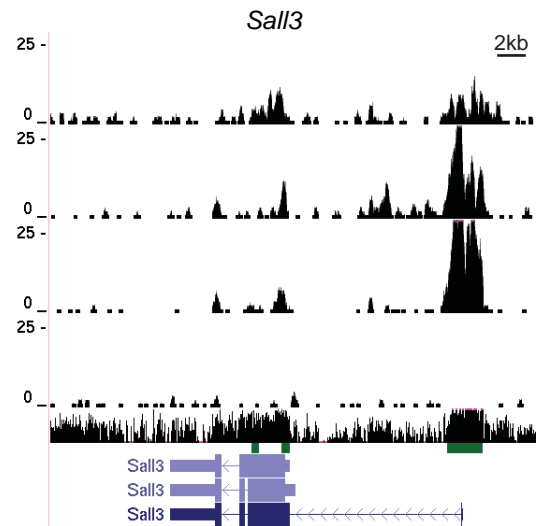
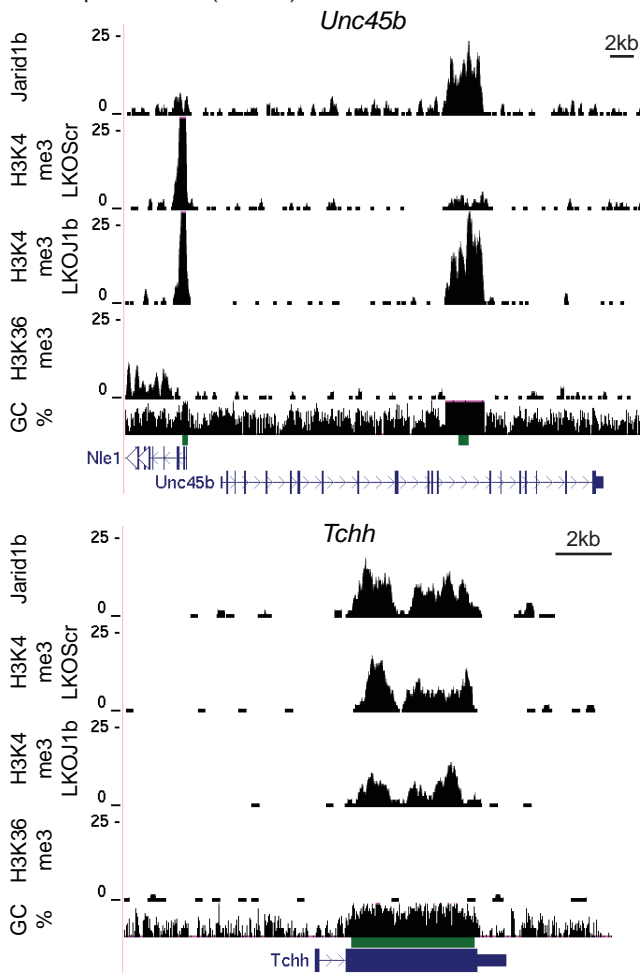


C

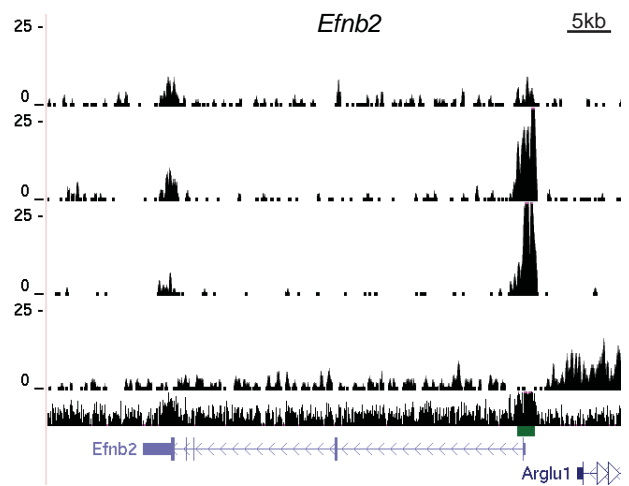
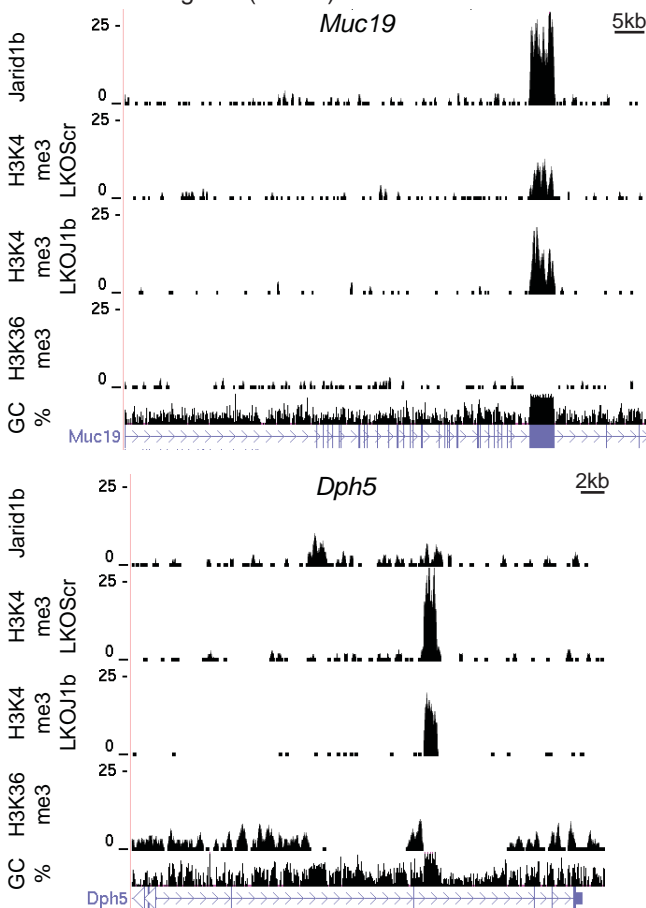
	LKO Scr	LKO Jarid1b
BrdU pos	28.2	27.5
G1	54.9	56.5
S	21.2	20.7
G2/M	23.9	22.8

Supplementary Figure 6. Proliferation and cell cycle progression are unchanged in Jarid1b knockdown NPCs. **(A)** Flow cytometry analysis of Scramble (LKO Scr), LKO Jarid1b and control NPCs pulsed with BrdU and stained with anti-BrdU antibody. Control represents cells without BrdU pulsing. **(B)** Cell cycle profile analysis by flow cytometry of LKO Scramble (Scr) and Jarid1b NPCs stained with PI (propidium iodide). **(C)** Quantification of results.

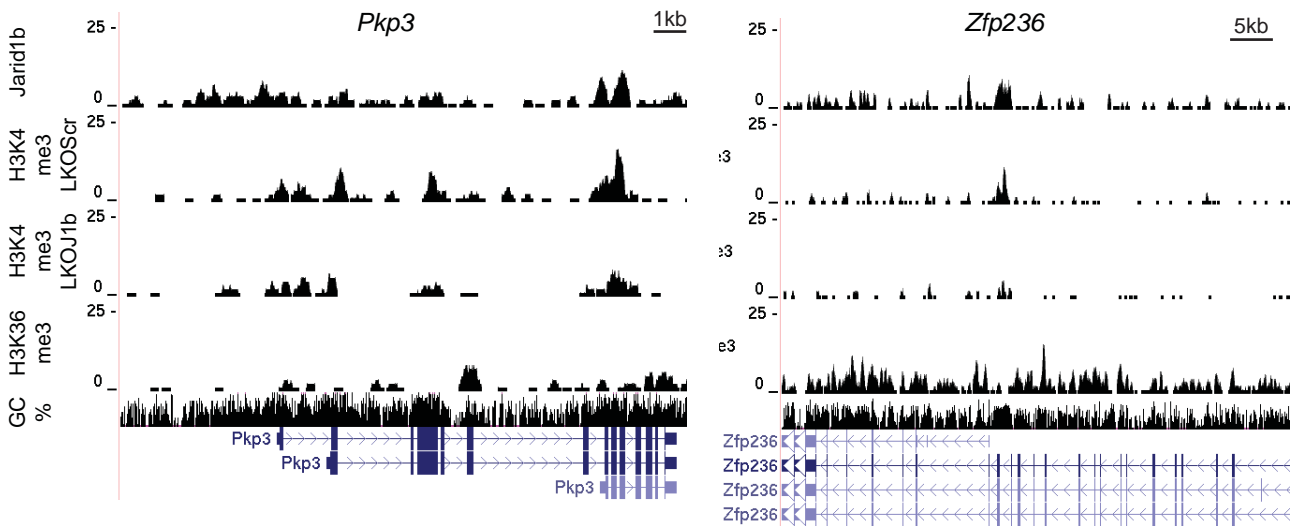
A CpG islands (22.4%)



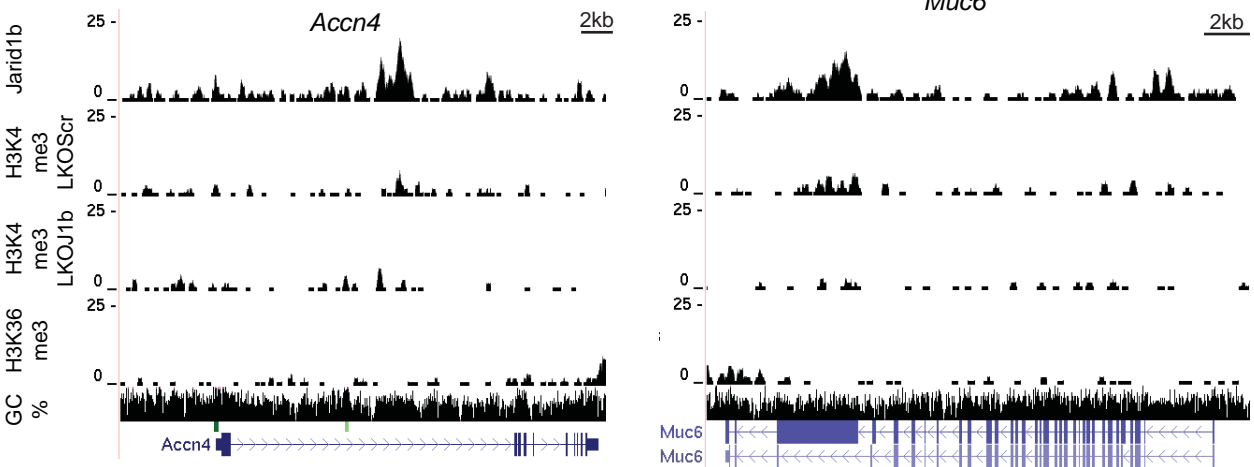
B GC rich regions (19.4%)



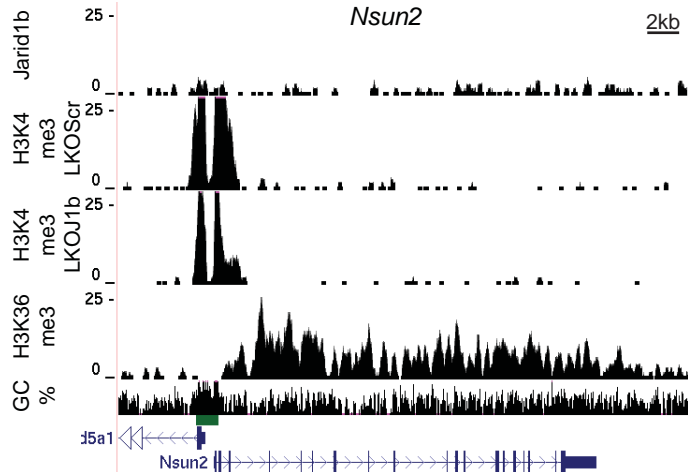
C Alternative transcription start sites (3.5%)



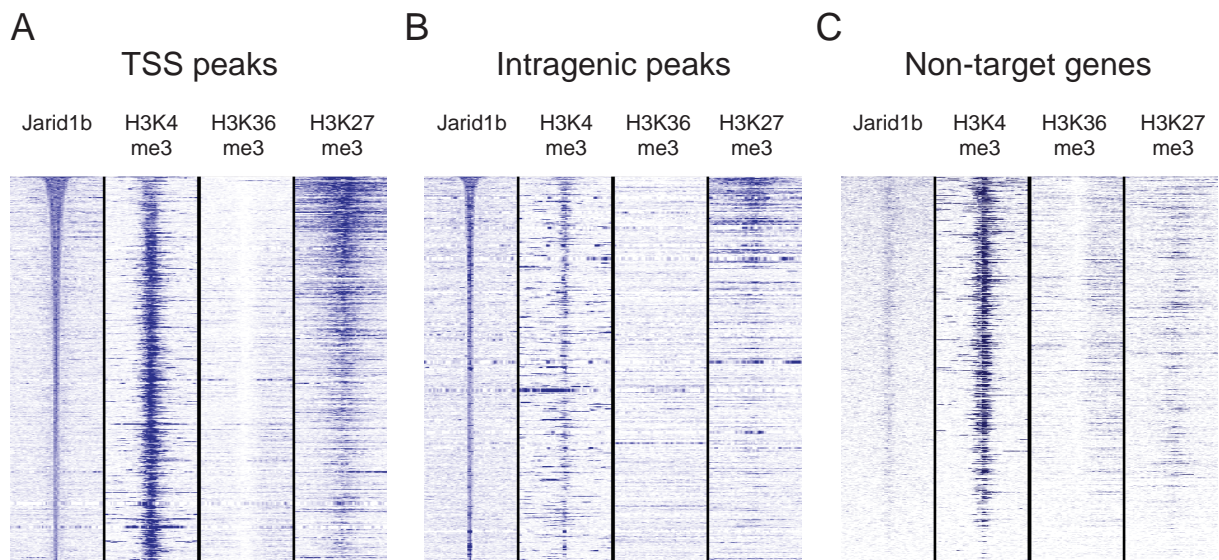
D No annotated sequence features



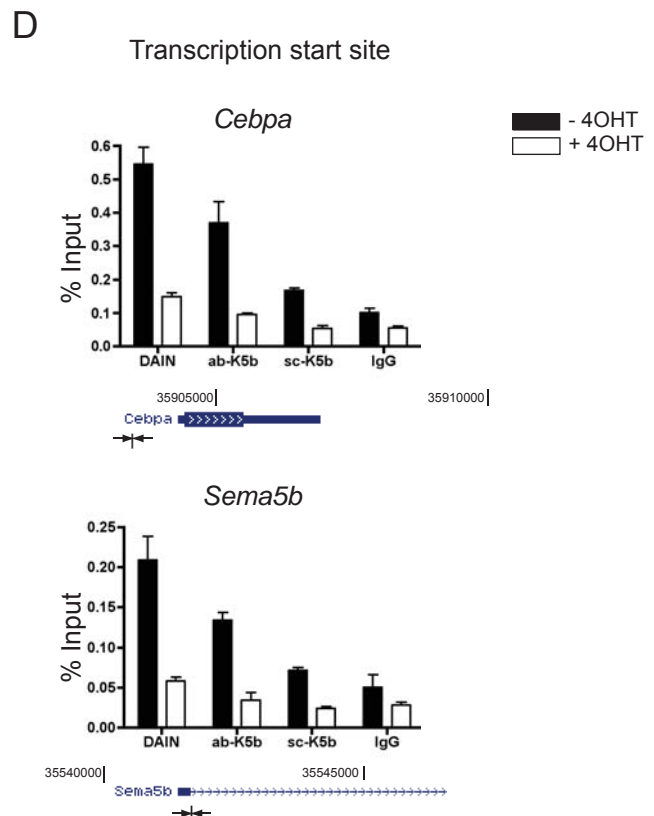
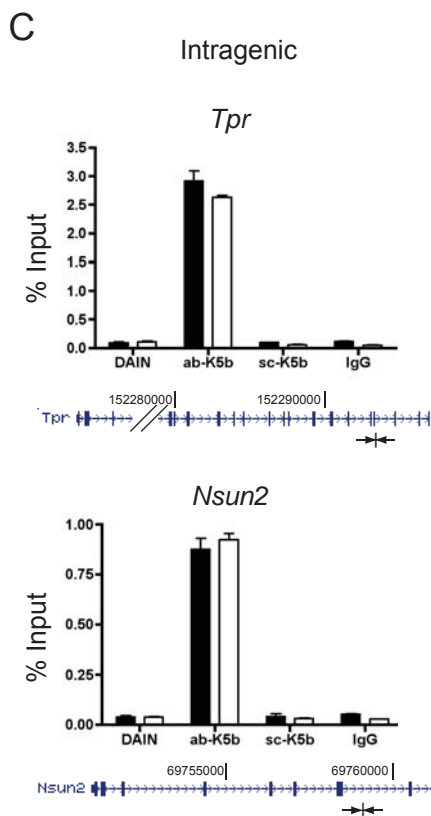
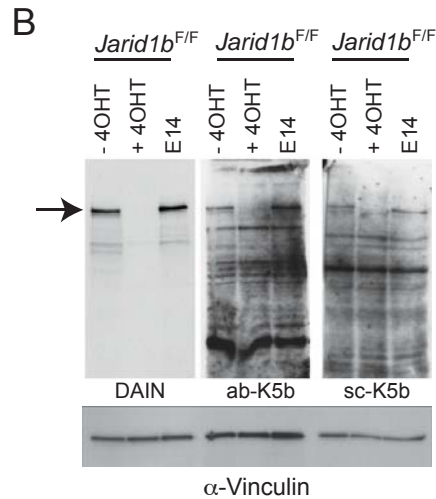
E Intragenic H3K36me3



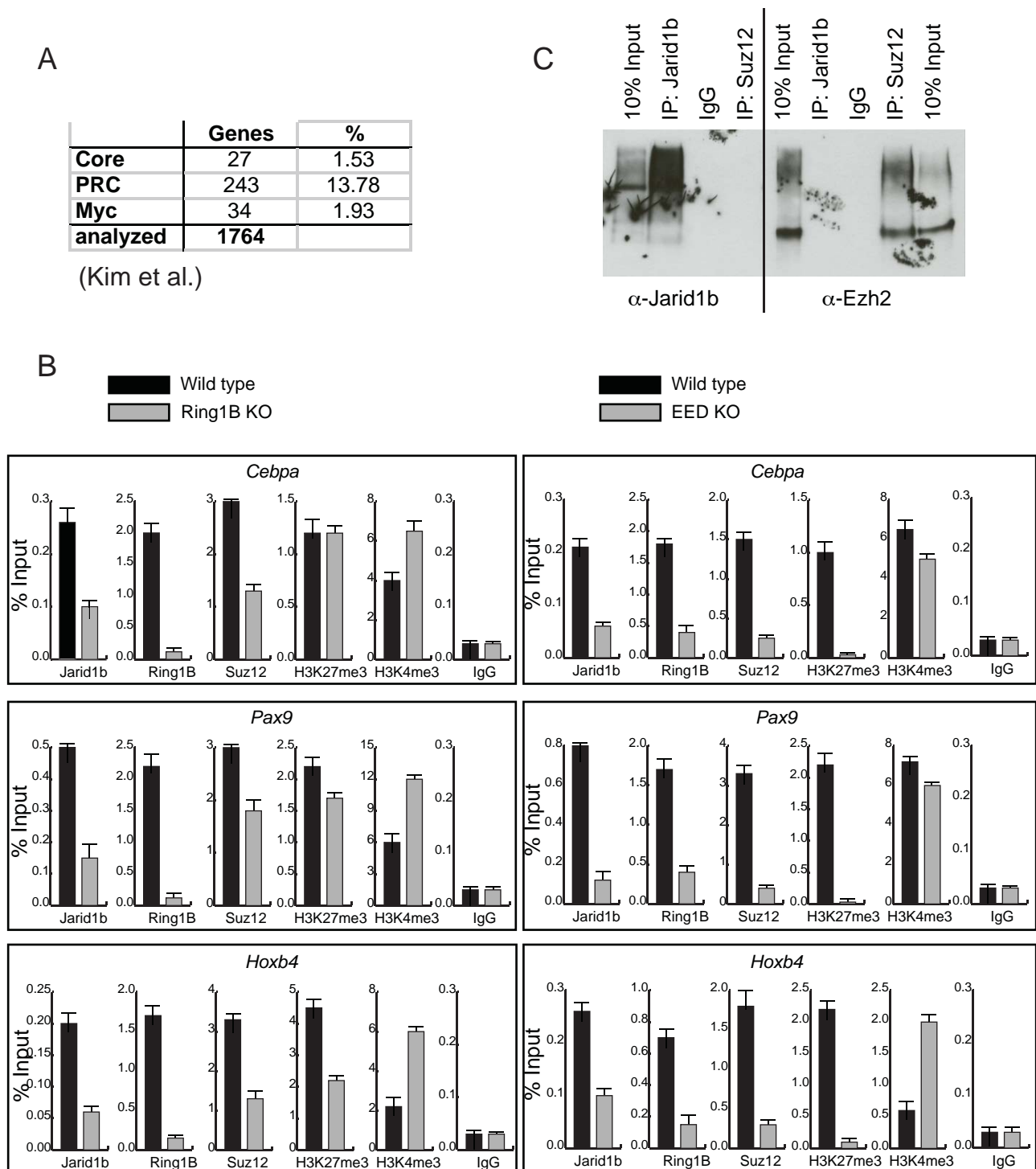
Supplementary Figure 7. Intragenic Jarid1b binding sites. Genome-wide binding profiles of Jarid1b and H3K4me3 in E14 mouse ESCs were determined by ChIP-sequencing. Genome-wide H3K36me3 profiles in ESCs were published by Mikkelsen et al (2007). Representative examples of Jarid1b binding profiles localized in intragenic regions that overlap (A) CpG islands, (B) other GC-rich regions or (C) alternative transcription start sites are presented. (D) Other intragenic Jarid1b peaks do not overlap any annotated sequence features. (E) Representative gene with intragenic H3K36me3 lacking Jarid1b binding. y-axis denotes number of sequence tag reads. The track for GC percentage is shown under each gene. Schematic presentation of Refseq transcripts is in dark blue and of alternative transcripts in light blue. Dark green bars represent CpG islands.



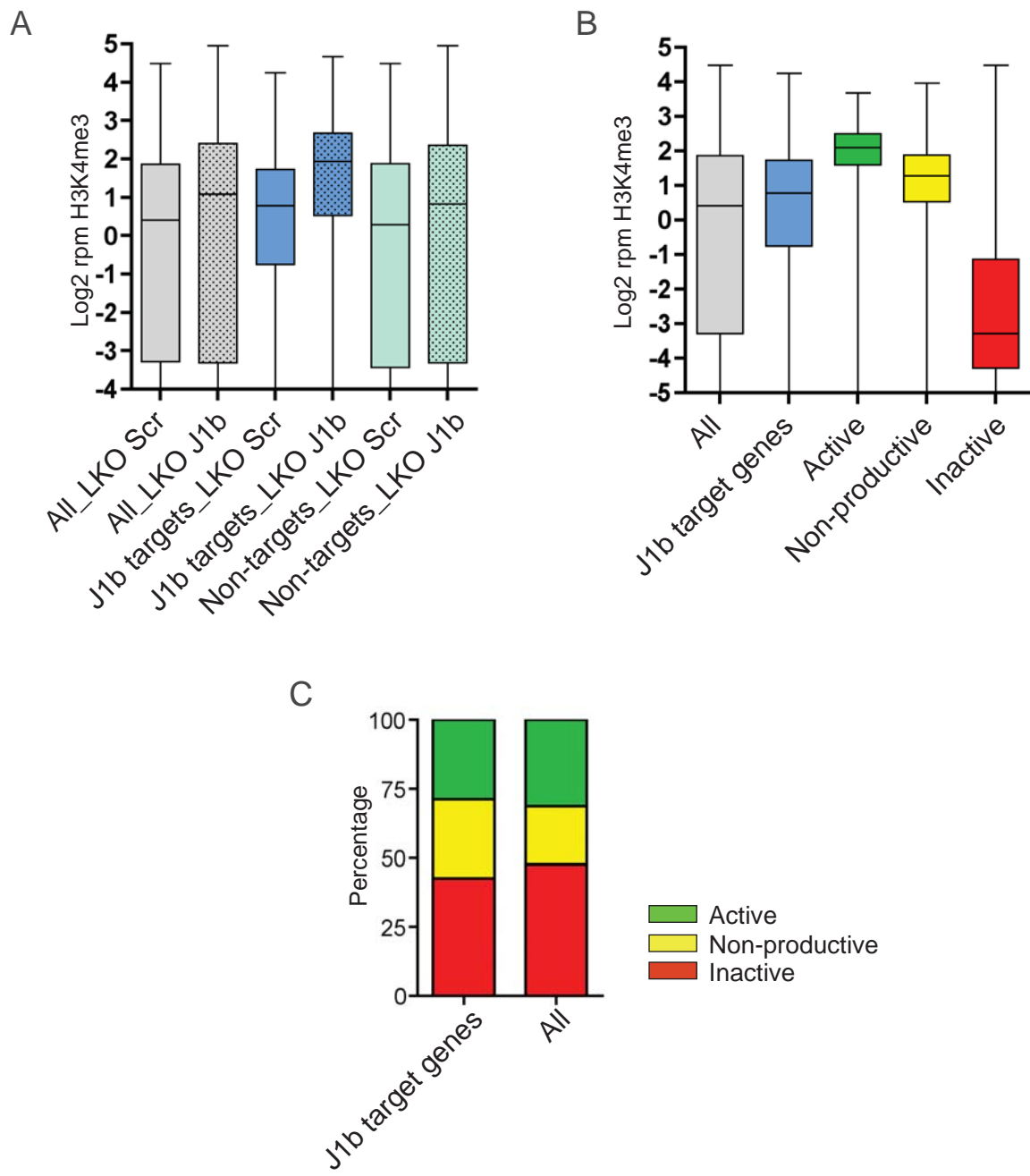
Supplementary Figure 8. Comparison of Jarid1b binding to histone methylation profiles. Genome-wide binding profiles of Jarid1b and H3K4me3 in E14 mouse ESCs were determined by ChIP-sequencing. Genome-wide H3K27me3 and H3K36me3 profiles in ESCs were published by Mikkelsen et al (2007). Heat maps for regions \pm 5 kb centered around Jarid1b peaks located (**A**) at the transcription start site (TSS) and (**B**) in intragenic regions were compared to H3K4me3, H3K36me3 and H3K27me3 profiles. (**C**) One thousand randomly chosen non-target genes are presented as control. Non-target genes are centered around the TSS (\pm 5 kb). Genes were sorted based on average Jarid1b tag density. Plots were generated using seqMINER.



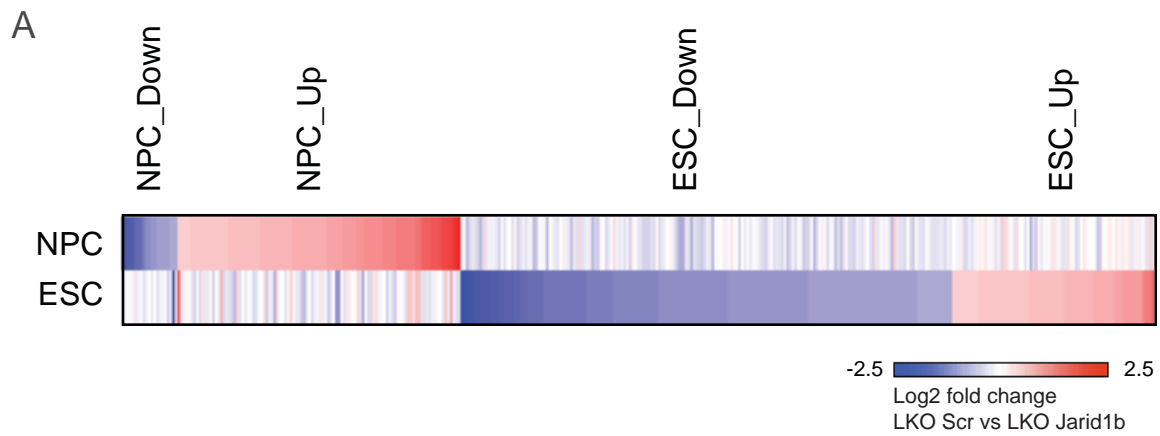
Supplementary Figure 9. Specificity of Jarid1b antibodies. (A) Schematic overview of antigens used to generate antibodies against Jarid1b (DAIN: antibody generated in this study; ab-K5b: anti-Jarid1b (Abcam, ab50958); sc-K5b: anti-Jarid1b (Santacruz, sc-67035)). (B) Immunoblotting of control (-4OHT), *Jarid1b* knockout (+4OHT) and E14 ESCs using the indicated Jarid1b antibodies. 20 μ g whole ESC lysate was used in all lanes and all samples were run on the same SDS-PAGE. Vinculin was used as loading control. (C, D) ChIP-qPCR using the indicated Jarid1b antibodies for intragenic regions (C) and around transcription start sites (D). Primer binding sites are illustrated below each panel.



Supplementary Figure 10. Jarid1b enrichment is reduced at target promoters in PcG knockout ESCs. **(A)** Numbers of Jarid1b target genes overlapping with three ESC regulatory modules (Core, Polycomb and Myc) (Kim et al, 2010). **(B)** ChIP-qPCR for Jarid1b, Ring1b, Suz12, H3K4me3, H3K27me3 in *Ring1b* (left panel) and *Eed* (right panel) knockout ESCs. Enrichment for histone marks was normalized to H3 levels. **(C)** Immunoprecipitation of either Jarid1b or Suz12 from ESCs followed by immunoblotting for Jarid1b and Ezh2.



Supplementary Figure 11. Jarid1b target genes carry intermediate levels of H3K4me3. H3K4me3 enrichment +/- 500 bp around all TSS was analyzed at different subsets of genes. **(A)** Comparison of H3K4me3 levels of all genes, Jarid1b targets and non-targets, in knockdown LKO Scramble (Scr) and LKO Jarid1b (J1b) ESCs. **(B)** H3K4me3 levels at TSS of Jarid1b target genes compared to all genes and gene sets divided according to their transcriptional activity (Rahl et al, 2010). **(C)** Classification of Jarid1b targets into groups according to their transcriptional activity (Rahl et al, 2010).

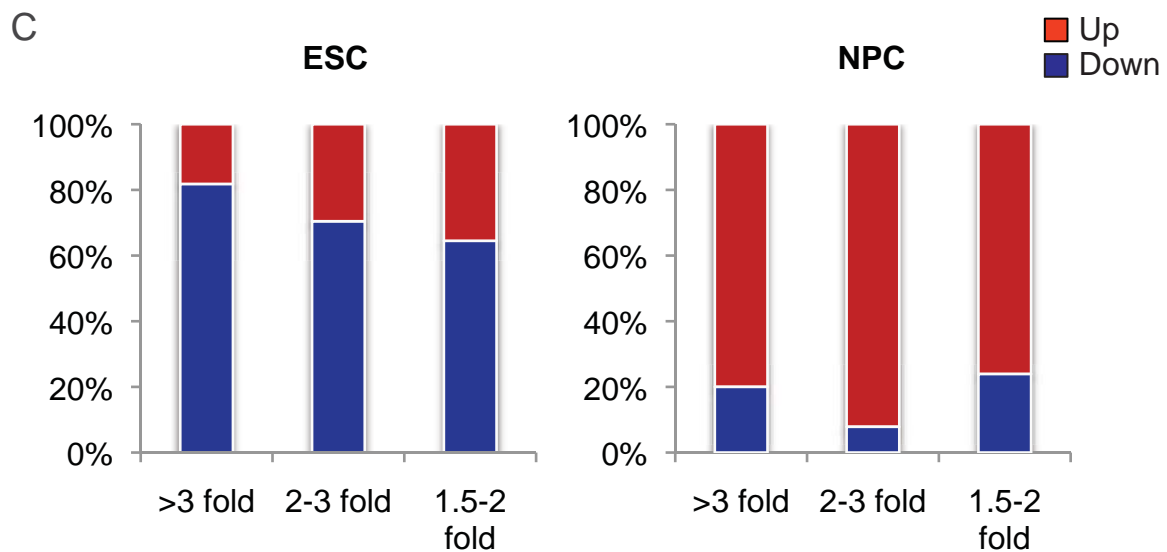


B

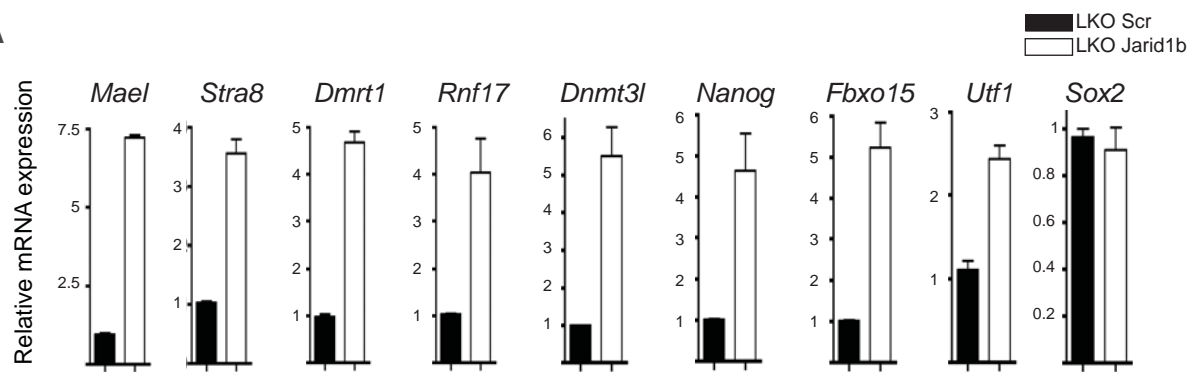
TOTAL	>3 fold	2-3 fold	1.5-2 fold
ESC	22	88	355
NPC	25	51	92

ESC	>3 fold	2-3 fold	1.5-2 fold
Up	4	26	126
Down	18	62	229

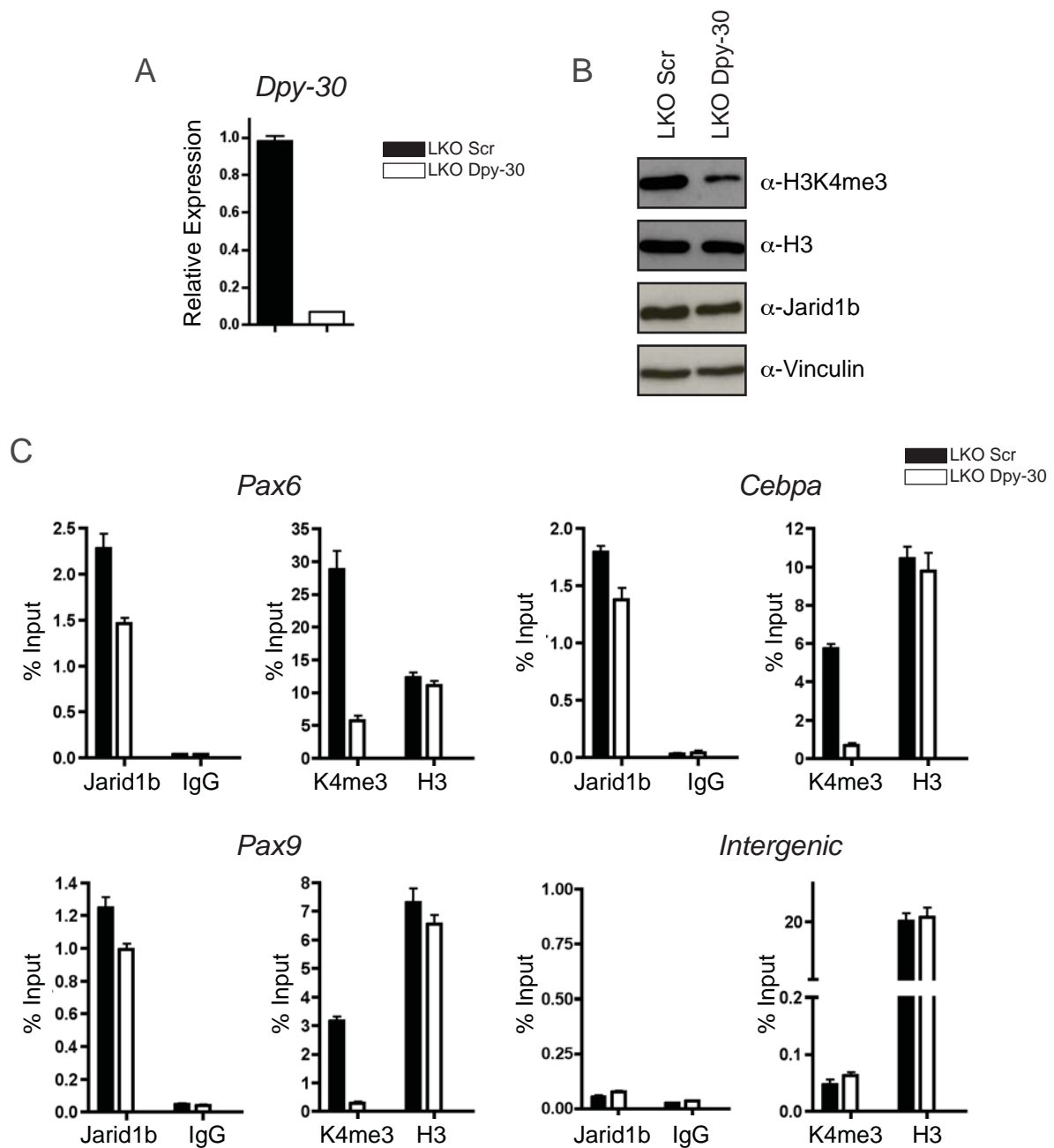
NPC	>3 fold	2-3 fold	1.5-2 fold
Up	20	47	70
Down	5	4	22



Supplementary Figure 12. Gene expression analysis of Jarid1b knockdown ESCs and NPCs. **(A)** Heatmap overview of genes down- (blue) or up- (red) regulated in Jarid1b knockdown versus scramble NPCs and ESCs. Coloring illustrates log₂ fold changes. **(B)** Number of genes differentially expressed in Jarid1b knockdown NPCs and ESCs compared to Scramble control, respectively. **(C)** Percentage of genes up- and downregulated in Jarid1b knockdown ESCs (left panel) and NPCs (right panel).

A

Supplementary Figure 13. Gene expression in Jarid1b knockdown NPCs. (A) Quantitative RT-PCR validation of expression changes of germ and stem cell genes in LKO Scr and Jarid1b knockdown NPCs (normalized to *Rplp0* levels).



Supplementary Figure 14. Jarid1b binding is reduced in Dpy-30 knockdown cells (A) Expression analysis of *Dpy-30* in stable lentiviral knockdown (LKO) Scramble (Scr) and Dpy-30 ESC lines determined by quantitative RT-PCR analysis (normalized to *Rplp0* levels). (B) Immunoblots of LKO Scr and Dpy-30 ESCs probed for H3K4me3, H3 (loading control), Jarid1b and Vinculin (loading control). (C) ChIP-qPCR for Jarid1b, IgG, H3K4me3 and H3 of Jarid1b target genes and a control region (intergenic) in LKO Scr and Dpy-30 knockdown ESCs.